APL Materials

RESEARCH ARTICLE | SEPTEMBER 11 2024

Comprehensive characterization of nitrogen-related defect states in β-Ga_2O_3 using quantitative optical and thermal defect spectroscopy methods

Hemant Ghadi ; Evan Cornuellue; Joe F. Mcglone ; Alexander Senckowski ; Shivam Sharma; Man Hoi Wong ; Uttam Singisetti ; Steven A. Ringel

APL Mater. 12, 091111 (2024)
https://doi.org/10.1063/5.0225570

Comprehensive characterization of nitrogen-related defect states in β-Ga_2O_3 using quantitative optical and thermal defect spectroscopy methods

Cite as: APL Mater. **12**, 091111 (2024); doi: 10.1063/5.0225570
Submitted: 25 June 2024• Accepted: 27 August 2024•
Published Online: 11 September 2024

Hemant Ghadi,[1,a)] Evan Cornuellue,[1] Joe F. Mcglone,[1] Alexander Senckowski,[2] Shivam Sharma,[3] Man Hoi Wong,[2] Uttam Singisetti,[3] and Steven A. Ringel[1]

AFFILIATIONS

[1]Electrical and Computer Engineering, The Ohio State University, Columbus, Ohio 43210, USA
[2]Electrical and Computer Engineering, University of Massachusetts Lowell, Lowell, Massachusetts 01854, USA
[3]Electrical Engineering, University of Buffalo, Buffalo, New York 14228, USA

[a)]Author to whom correspondence should be addressed: ghadi.1@osu.edu

ABSTRACT

This study provides a comprehensive analysis of the dominant deep acceptor level in nitrogen-doped beta-phase gallium oxide (β-Ga_2O_3), elucidating and reconciling the hole emission features observed in deep-level optical spectroscopy (DLOS). The unique behavior of this defect, coupled with its small optical cross section, complicates trap concentration analysis using DLOS, which is essential for defect characterization in β-Ga_2O_3. A complex feature arises in DLOS results due to simultaneous electron emission to the conduction band and hole emission to the valence band from the same defect state, indicating the formation of two distinct atomic configurations and suggesting metastable defect characteristics. This study discusses the implications of this behavior on DLOS analysis and employs advanced spectroscopy techniques such as double-beam DLOS and optical isothermal measurements to address these complications. The double-beam DLOS method reveals a distinct hole emission process at E_V+1.3 eV previously obscured in conventional DLOS. Optical isothermal measurements further characterize this energy level, appearing only in N-doped β-Ga_2O_3. This enables an estimate of the β-Ga_2O_3 hole effective mass by analyzing temperaturedependent carrier emission rates. This work highlights the impact of partial trap-filling behavior on DLOS analysis and identifies the presence of hole trapping and emission in β-Ga_2O_3. Although N-doping is ideal for creating semi-insulating material through the efficient compensation of free electrons, this study also reveals a significant hole emission and migration process within the weak electric fields of the Schottky diode depletion region.

Extrinsic dopant incorporation in semiconductors controls the Fermi-level position in the bandgap, resulting in conductive or semi-insulating epilayers/substrates.[1–3] In beta-phase gallium oxide (β-Ga_2O_3), which possesses inherent n-type conductivity, impurities such as Si, Ge, and Sn are common donors that efficiently create free electrons and n-type conductivity due to the shallow nature of their energy levels in the bandgap.[1–4] In contrast, impurities such as nitrogen,[5] iron,[6] magnesium,[1] cobalt,[7] and nickel[8] are theoretically and experimentally verified to introduce acceptor-like bandgap states in β-Ga_2O_3 that are very deep in the bandgap at E_C-2.9 eV, E_C-0.8 eV, E_C-3.8 eV, E_C-1.9 eV, and E_C-2.2 eV, respectively. These deep acceptor states can compensate for excess electrons and pin the Fermi level at the deep acceptor energy level, thus creating highly resistive or semi-insulating layers necessary for high breakdown and radio frequency (RF) β-Ga_2O_3 devices. Our prior work investigated energy levels associated with N doping by deep-level optical spectroscopy (DLOS) since it is an intriguing and promising deep acceptor candidate.[5] Nitrogen doping in β-Ga_2O_3 is highly stable due to its 3.87 eV barrier diffusion activation energy[1,9] and its primary acceptor energy at ~E_C-2.9 eV as predicted by theoretical calculations for the oxygen site III (N_{OIII}), which DLOS corroborated.[5] However, a complicating factor created for DLOS characterization

when states are below half of the bandgap ($E_G/2$) for n-type material is that incoming photons can cause electron photoemission to the conduction band and competing hole emission (electron capture from) to the valence band.[10] If not accounted for, this competition makes determining the accurate concentration of such defect states via DLOS difficult, and it can even change the sign of the measured steady-state photocapacitance (SSPC) depending on which process is dominant. In conventional semiconductors such as GaN, negative excursions in the SSPC due to states below midgap can be easily attributed to hole emission to the valence band and subsequent hole collection.[10,11] However, for β-Ga_2O_3, free holes are relatively immobile and are immediately captured through self-trapping (which leads to its lack of p-type conductivity).[12–14] Our prior published work on the E_C-2.9 eV (N_{OIII}) acceptor state circumvented this issue by using a +0.7 V forward bias filling pulse during the trap filling stage of the DLOS measurement to ensure complete saturation of this state by electrons through the current injection.[5] Conventional DLOS measurements using a 0 V filling bias pulse revealed behavior suggesting that both conduction band and valence band emission/capture processes from the same E_C-2.9 eV state are present despite the lack of p-type conductivity. Thus, the purpose of this work is to explore and resolve this possible dual-band behavior in significant detail using a method known as double-beam DLOS.[10,15,16] Various pump–probe combinations of light source energies are used to isolate and then quantify both electron and hole emission processes related to the N_{OIII} defect. This study aims to offer new fundamental experimental data on conduction and valence band processes originating from deep states in β-Ga_2O_3. This analysis is crucial for accurately interpreting DLOS data and understanding the photophysics related to these processes in β-Ga_2O_3.

The dual beam DLOS studies were conducted on the samples we characterized in our prior work.[5] Briefly, halide vapor phased epitaxial (HVPE) grown β-Ga_2O_3 samples[17] with a background Si doping of 1.2×10^{17} cm^{-3} were implanted with N to create a uniform N concentration of 2×10^{16} cm^{-3} for a thickness of 1 μm.[5,9] The N-implanted sample was annealed at 1100 °C for 10 mins in N_2 ambient for N acceptor activation. Subsequently, 8 nm thick semi-transparent Ni-Schottky diodes were fabricated using a two-step lithography process, and an ohmic stack of Ti/Al/Ni/Au was deposited on the back side of the conductive substrate.[5,18–21] The extracted doping concentration from capacitance–voltage (CV) characteristics was ~1.2×10^{17} cm^{-3}, consistent with the background Si. With the addition of N co-doping, the CV net doping reduced to a value of $0.9–1 \times 10^{17}$ cm^{-3}, moving the calculated Fermi level to ~0.1 eV below the conduction band. While the DLOS

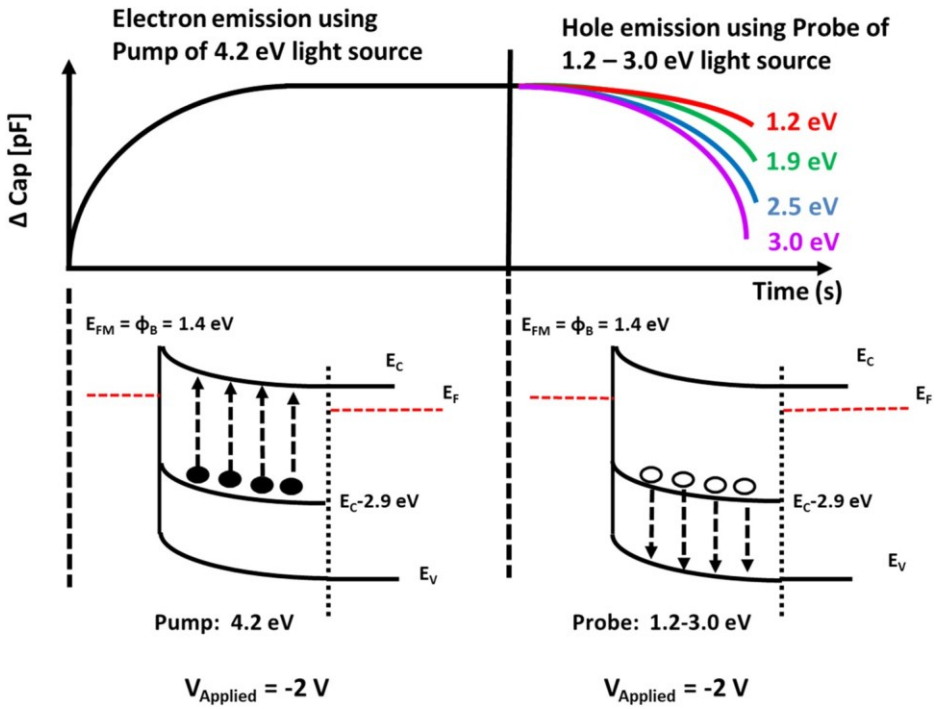

FIG. 1. Schematic of a double beam DLOS experiment showing the light source (pump = 4.2 eV) emitting the nitrogen-related level with a corresponding increase in ΔC and the second monochromatized light source (probe = 1.2–3.0 eV) for the hole emission process/trap refilling causing a decrease in ΔC. The corresponding band diagram illustrates the emission process from the defect state at the pump and probe processes.

technique has been explained previously, the double-beam DLOS method is less known and is described herein. Conducted at a constant temperature of 305 K, the first step is to fill all defect states using a forward bias

pulse of 1.5 V for 600 s. This causes a 2 mA current to flow through the Schottky diode, saturating the traps with electrons. As discussed earlier, a higher current value for the experiment is selected to ensure all defect levels are completely filled with electrons via current injection. After applying the fill pulse, an immediate reverse bias of −2 V was applied while illuminating light through the semi-transparent Ni Schottky metal using a 9 W 4.2 eV UV-LED light source (pump). The light source emits electrons to the conduction band from all states whose energy levels are less than 4.2 eV below the conduction band edge, including the N state at E_C-2.9 eV. The higher energy light source was selected such that the entire spectrum of the optical cross section[22,23] for this N state is excited,[5] yet at an energy level low enough so that it does not result in electron emission from the commonly reported E_C-4.4 eV defect state based on the detailed optical cross section analysis of this state from our prior work.[20] The pump source was deactivated upon complete emission of the E_C-2.9 eV state, confirmed by observing saturation of the emission transient, followed by subsequent illumination using the probe light. The optical probe source was facilitated using a 450 W Xe-Arc lamp light dispersed through a monochromator to vary the probe photon energy from 1.2 to 3.0 eV in increments of 0.05 eV. During the probe process, the diode was maintained at a constant reverse bias of −2 V and was repeated for each probe energy step. The subsequent photocapacitance transient for each probe energy was digitally recorded. A schematic of the dual beam DLOS experiment is shown in Fig. 1, along with the corresponding band diagrams to help visualize the assumed electron and hole emission processes that the subsequently described experimental results will verify. The sign of the transient allows the differentiation between electron emission to the conduction band (i.e., a positive transient due to an increase in positive space charge) and hole emission to the valence band (i.e., a negative transient due to an increase in negative space charge). In the double beam DLOS measurements, the electron emission dominates during the pump process, followed by hole emission to the valence band during the probe process. The entire process is schematically depicted in Fig. 1.

The difference in the sign of the photocapacitance transients will manifest in the SSPC spectrum. Before describing the doublebeam DLOS results, it is helpful to show this effect on the SSPC response, especially as it motivates why both conduction and valence band processes must be investigated. Figures 2(a) and 2(b) compare the SSPC spectra measured using conventional methods with a 0.7 and 0 V fill pulse bias, respectively, followed by the spectrally resolved photoemission experiment at a −2 V reverse bias. With forward bias fill pulse, we are forcing all defect levels to fill through the current injection, and the DLOS results have been published in Ghadi *et al.*[5] Both positive and negative photocapacitance onsets are observed in Fig. 2(b), indicating interaction with the conduction and valence band, respectively, when using a 0 V fill pulse bias. The positive onsets are due to electron photoemission (increase in positive space charge) to the conduction band, and the negative onsets are due to hole emission (increase in negative space charge) to the valence band. The positive onsets seen at 2.3 and 3.4 eV photon energies in both Figs. 2(a) and 2(b) are from the E_C-2.0 eV and E_C-2.9 eV defect levels emission previously reported.[5] The former has been found to possess a Franck–Condon energy (D_{FC}) of 0.5 eV[20] and has been associated with the predicted $2V_{Ga}$-Ga_i defect level.[19,20,24–26] The latter positive SSPC onset at E_C-3.4 eV has also been studied and is due to the N_{OIII} state at E_C-2.9 eV with a D_{FC} = 1.4 eV.[1,5] However, the SSPC spectrum measured with a 0 V fill pulse reveals the presence of negative onsets, a large one that initiates near photon energy of 2.5 eV and a smaller one near 1.5 eV, which are of primary focus here. As described above, such photocapacitance behavior can only be associated with an increase in negative space charge, and so this warrants deeper investigation with the aforementioned dual beam DLOS.

Figure 3(a) shows room temperature (305 K) double-beam DLOS experimental results. The negative slope of the recorded photocapacitance transients during the probe measurement is consistent with increasing negative space charge due to hole emission. The large timescale on the x-axis indicates that these are very slow transients, and this is consistent with a high hole effective mass,

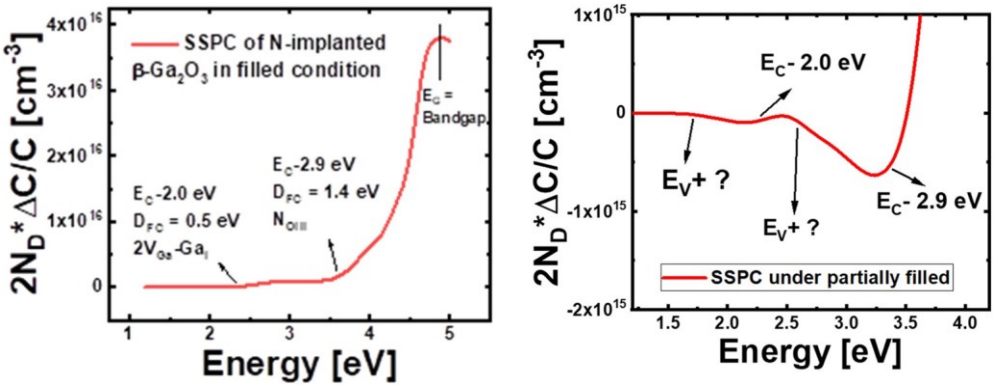

FIG. 2. SSPC results using (a) the 0.7 V filling pulse voltage reported by Ghadi *et al.*[5] and (b) the standard 0 V filling pulse voltage. The two positive onsets indicated are due to electron photoemission to E_C from defect energy levels at E_C-2.0 eV and E_C-2.9 eV determined from optical

cross section analysis as reported in Ghadi *et al.*,[5] while the two negative onsets denoted by E_V+? in (b) in the measured SSPC imply hole emission processes to E_V.

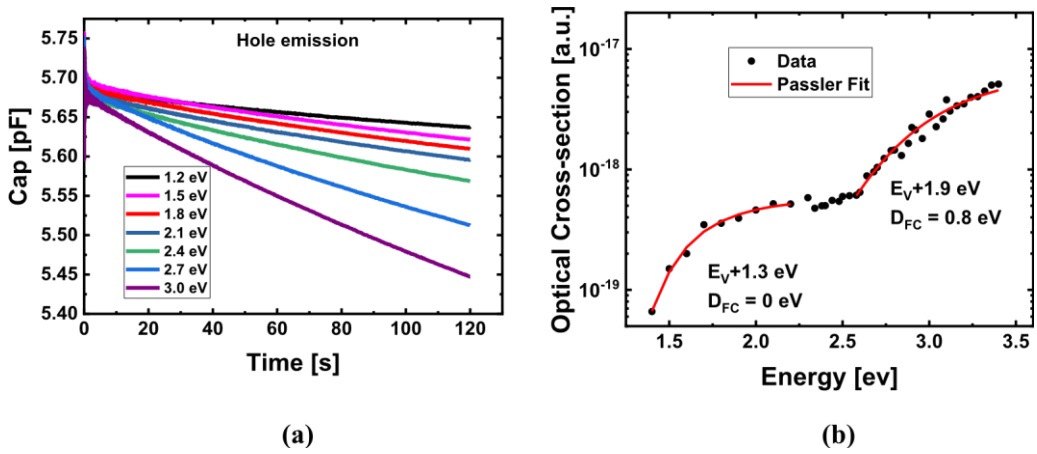

FIG. 3. (a) Measured negative capacitance transient from the hole emission process using the double beam DLOS measurements (probe). (b) Extracted optical cross section from the negative transients exhibiting two distinct onsets when fitted to the Passler model[22] results in two defect states at E_V+1.3 eV (D_{FC} = 0) and E_V+1.9 eV (D_{FC} = 0.8 eV), respectively.

noting that it is only because of the drift field in the Schottky barrier depletion region that any hole collection is possible. Such observations of hole transport due to a drift field have been previously reported for β-Ga_2O_3 photodetectors.[27,28] A simple analytical model was developed to substantiate this further as part of this work. The model utilizes the electric field calculated by solving the Poisson equation to extract the hole drift velocity, assuming the reported hole mobility value of 10^{-6} cm^2/V-s.[29] The travel time is calculated by integrating the velocity over the depletion region. This model reveals that ~50 ms would be required to allow a photogenerated hole to drift across the depletion region and be collected for a drift field of 0.01 MV/cm. In our double-beam experiments, we applied a minimum electric field of 0.08 MV/cm across the depletion region. In addition, we measured transients over 100 s to ensure the collection of photoemitted holes.

From the photocapacitance transients, the optical cross sections associated with the hole emission transients could be extracted, as shown in Fig. 3(b). Two distinct states are immediately evident, one with a relatively sharp onset starting around 1.3 eV and saturating near 2 eV and one with a broader onset that starts around 2.6 eV. A sharp onset indicates a low D_{FC} energy, implying negligible local lattice relaxation associated with that defect, thus leading to similar emission energies for optical and thermal transitions. In contrast, a broad onset usually indicates a substantial D_{FC} linked to local lattice relaxation.[22,23] Consequently, the optical transition occurs at the sum of thermal transition energy and high D_{FC}.[30] Therefore, the optical cross section should be modeled using either the Passler model[22] or the Chantre Vincent and Bois (CVB)[23] model to extract energy levels, as they incorporate Frank–Condon energies accurately.

The optical cross sections for these two hole emission states were fitted to the Passler model to extract the precise trap and Franck–Condon (D_{FC}) energies.[22] The extracted energies correlate with the negative going excursions in the SSPC discussed earlier in Fig. 2(b). The two different energy levels are derived from fitting and are located at E_V+1.3 eV (D_{FC} = 0 eV) and E_V+1.9 eV (D_{FC} = 0.8 eV). The E_V+1.9 eV position in the bandgap lines up remarkably close to the E_C-2.9 eV state revealed by electron photoemission to the conduction band (i.e., 1.9 eV + 2.9 eV = 4.8 eV bandgap) that has been attributed to N_{OIII}, and perhaps this is the same defect level.[5] The level at E_V+1.3 eV, which is also implied by the slight negative slope of the SSPC data in that energy range from Fig. 2(b), needs further investigation. Interestingly, its modeled D_{FC} is 0 eV, suggesting insignificant lattice relaxation. Similar to the E_C-2.9 eV/Ev+1.9 eV level, we have only seen evidence for the E_V+1.3 eV state for β-Ga_2O_3 doped with N (including not being observed in samples subjected to damage via high energy particle irradiation),[5,19,31] suggesting a possible association with an N-related defect.

We can now focus on defect concentrations of these levels based on their communication with the valence band. Figure 4 shows the comprehensive pump–probe process, allowing the direct and independent interrogation of electron and hole emission using double-beam DLOS coupled with a laser source. Figure 4(a) shows the 4.2 eV pump process that emits all trapped electrons from any state within 4.2 eV from the conduction band after the electrical electron filling pulse, including both E_C-2.9 (E_V+1.9 eV) and E_V+1.3 eV states. Subsequently, Fig. 4(b) shows the probe results that can isolate and quantify the hole emission processes via two laser sources. The laser sources are selected such that a higher photon

flux, i.e., several orders higher than a xenon arc lamp, expedites the emission process. Based on the optical cross section results from Fig. 4(b), only holes from the E_V+1.3 eV state will be completely emitted using a red laser probe source (1.8 eV), while both the E_V+1.3 eV and E_V+1.9 eV states will emit holes using a purple laser probe (3.1 eV) source. The measured trap concentrations of E_V+1.3 eV and E_V+1.9 eV states based solely on saturating the hole emission were 3.1×10^{15} and 1.74×10^{16} cm^{-3}, respectively. Considering the E_v+1.9 eV state, this concentration is very close to the trap concentration obtained solely based on electron emission to the conduction band at E_C-2.9 eV, with both matching the N concentration from SIMS, providing strong evidence that, indeed, this is the same N state

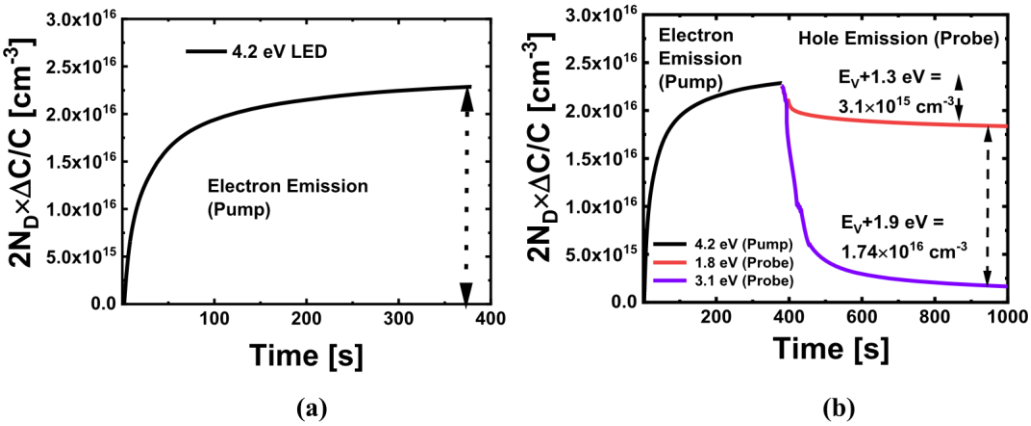

FIG. 4. (a) Majority carrier emission process accomplished using a pump light source representing the electron emission process (emptying the state). The trap concentration measured as a function of time closely matched the 2×10^{16} cm^{-3} implanted nitrogen concentrations measured from SIMS. (b) Minority carrier emission process (refilling with electrons resulting in hole emission) with two specific laser sources (probe) for precisely measuring the hole trap concentrations described in the double beam DLOS. The measured trap concentrations from electron and hole emission processes perfectly matched.

that is also the primary source of carrier compensation that we have earlier demonstrated.[5]

With the E_v+1.9 eV state appearing to be satisfactorily associated with the E_C-2.9 eV level attributed to N_{OIII}, and with the concentration of the state closely matching between both electron emission and hole emission DLOS measurements,[5] further characterization of the E_v+1.3 eV state is necessary to gain a complete understanding of the DLOS behavior for N doped β-Ga_2O_3. To accomplish this, we have employed an optical isothermal defect spectroscopy method. This spectroscopy combines double-beam DLOS spectroscopy and conventional thermal DLTS measurements. Optical isothermal spectroscopy has certain limitations and can only be used to characterize defect states closer to either of the bands. Since E_V+1.3 eV is relatively close to the valence band and its thermal emission time constant can be extracted within the temperature range of our DLTS measurement, characterization of this defect level by optical isothermal DLTS is viable. Using the 4.2 eV pump light source to empty electrons from this state as an effective "hole filling pulse," subsequent isothermal DLTS can then be used to emit holes and monitor this effect on the resultant thermal capacitance transient, similar to a standard DLTS experiment. The hole thermal emission process is immediately measured after turning off the 4.2 eV light source (i.e., hole-filling pulse). A schematic of optical isothermal measurement is shown in Fig. 5(a) to visualize the process. After the electron emission process to the conduction band, the occupancy of both E_C-2.9 eV/E_v+1.9 eV and E_v+1.3 eV defect states change because the trapped electrons have been optically emitted to the conduction band, and this "empty electron" condition is maintained by virtue of the measurement occurring in the depletion region, where there are no free electrons for re-capture. However, the trapped hole or empty electron state would have thermal emission rates that are exponentially dependent on temperature, i.e., increasing the temperature can expedite the emission if this process is genuinely occurring and can be measured by DLTS. Hence, the optical isothermal measurements were conducted between 415 and 450 K in steps of 5 K to expedite the thermal emission process. The raw transients measured from isothermal experiments are exponentially decaying, and a graph of individual time constants obtained from the boxcar integrator applied to the capacitance transients at each temperature is shown in Fig. 5(b). The method for extracting and analyzing the time constants is explained in Turchanikov *et al.*[32] The temperature range was chosen due to the maximum temperature limits of our probe station (450 K) and a practical lower limit to ensure that the hole emission time constant could be measured within a reasonable time window. Again, emission from the E_v+1.9 eV state is not observable in this temperature range since it is too far from the valence band to be thermally ionized.

The analyzed spectra are plotted similarly to conventional DLTS spectra with a time constant (1/emission rate) and temperature as variables shown in Fig. 5(b). The measured peaks at specific temperatures were fitted to an Arrhenius plot shown in Fig. 5(c), and the obtained trap energy of E_V+1.27 eV closely matches what was observed using double-beam DLOS measurement, consistent with D_{FC} = 0 eV that predicts the optical and thermal emission energies would be nearly identical as noted earlier. From the optical

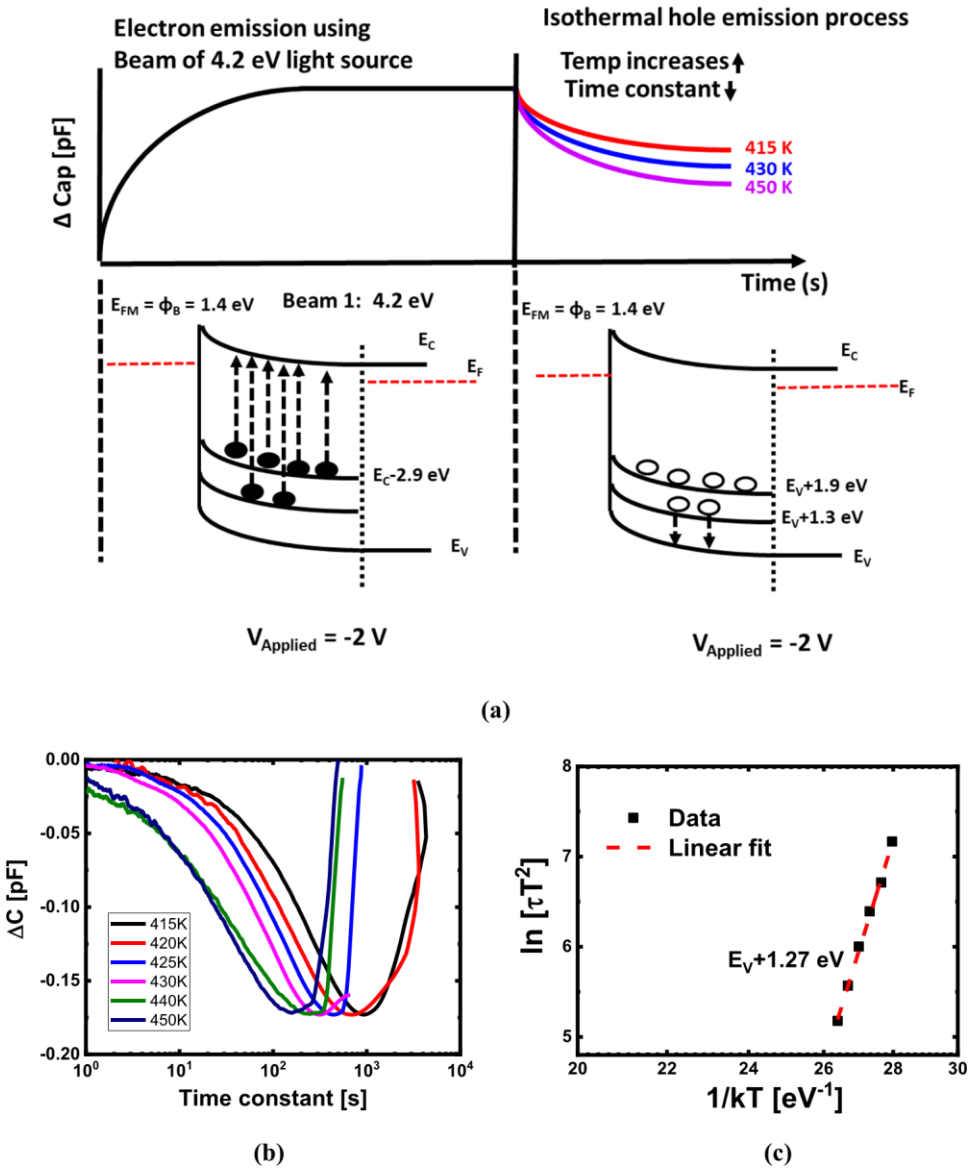

FIG. 5. (a) Optical isothermal emission schematic showing the thermally stimulated emission process used to detect the E_V+1.3 eV state instead of a secondary light source (probe), along with illustrative band diagrams showing the optical and thermal emission processes. (b) Capacitance plotted similarly to DLTS spectra as a function of derived time constants from the boxcar integrator at various temperatures. (c) The resultant Arrhenius plot from the peak positions enables the extraction of the corresponding trap

isothermal DLTS measurements, the trap concentration of the E_V+1.3 eV state was found to be 3.3×10^{15} cm^{-3}, matching the double beam DLOS results, establishing self-consistency between these very different thermal and optical measurement methods. Interestingly, the x-intercept from the Arrhenius plot can be used to estimate the hole-effective mass, as follows:[33]

$$\ln\left(\frac{T^2}{e_h}\right) = \frac{(E_V \pm E_T)}{k_b T} - \ln(\sigma_p \gamma_p). \quad (1)$$

Here, T is the temperature, e_h is the hole emission rate, k_b is the Boltzmann constant, σ_p is the hole thermal cross section, and γ_p is a constant defined by hole thermal velocity and hole density of states. Based on the slow hole emission properties, assuming a typical range of hole capture cross section values of $\sim 10^{-15}$–10^{-17} cm^2, the resultant calculated hole effective mass range from this analysis would

energy, which matches the value obtained from the double-beam DLOS experiment.

be (40–1000) × m_o. These values are consistent with the theoretical calculations.[34–38] It is worth noting again that DLTS detection of a hole trap is possible because the experiment occurs within the depletion region electric field.

In addition, to demonstrate that hole emission from E_V+1.3 eV is only observed after N-doping and is related to N, we performed double-beam DLOS on the HVPE sample without nitrogen implantation, illustrated in Fig. 6. The DLOS spectra and the summary of the defect states have been reported previously.[5] The double beam experiment was performed with the pump source photon energy maintained at 4.2 eV while the probe source energy was applied for photon energies of 1.9 and 3.0 eV. As shown in Fig. 6, no hole emission was observed, which is in contrast to the strong hole emission transients for the N-doped samples shown earlier in Fig. 4(b). This comparison of double-beam DLOS results for HVPE materials with and without N doping demonstrates that this hole emission process at E_V+1.3 eV is due to N doping.

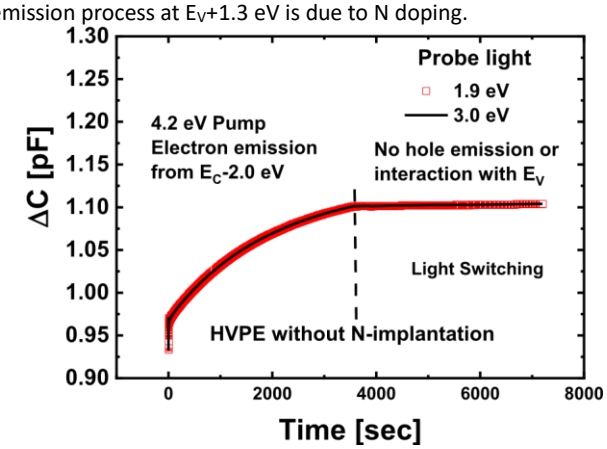

FIG. 6. Electron emission from E_C-2.0 eV was accomplished with a pump source of 4.2 eV, shown on the left side of the dashed vertical line. Switching from the pump to the 1.9 and 3.0 eV probe source on the right side of the dashed vertical line did not result in negative transients, indicating that no hole emission is observed without N doping for these samples.

In conclusion, this study comprehensively explains the dominant N deep acceptor level created in N-doped β-Ga_2O_3. It elucidates and reconciles the observed hole emission features in DLOS, attributing them to measurements conducted within the depletion region under electric fields. Both electron emission from E_C-2.9 eV and hole emission from E_V+1.9 eV appear to stem from the same energy level, identified as N_{OIII} in nitrogen-doped β-Ga_2O_3, the primary source of carrier compensation for N-doped β-Ga_2O_3. Optical cross section analysis reveals a high D_{FC} associated with both electron emission (1.4 eV) and hole emission (0.8 eV) from the same energy level, suggesting the presence of two distinct atomic configurations. Double beam experiments accurately pinpoint the defect location in the bandgap and enable quantitative characterization of emission processes associated with both conduction and valence bands. Furthermore, these experiments revealed an unexpected state at E_V+1.3 eV that was thoroughly investigated through double-beam DLOS and optical isothermal measurements. A zero D_{FC} energy associated with the E_V+1.3 eV defect level suggests no lattice distortion or a nearly flat valence band transition. The nearly perfect match between the energy level calculated from double-beam DLOS and the optical isothermal spectroscopy further supports this conclusion. This specific state has been exclusively observed in N co-doped β-Ga_2O_3, strongly suggesting its association with nitrogen.

The authors acknowledge the work of Ohio State Ph.D. student Tal Kasher for his support in device fabrication. The authors acknowledge the funding from the Air Force Office of Scientific Research (AFOSR) GAME-MURI (Grant No. FA9550-18-1-0479) (Ali Sayir, Program Manager), AFOSR (Grant No. FA9550-22-1-0527), and the U.S. Air Force Radiation Effects Center of Excellence (Grant No. FA9550-22-1-0012). This work was supported, in part, by the Ohio State University Institute for Materials and Manufacturing Research. The authors also want to acknowledge NSF under Award Nos. ECCS 2019749, 2231026, and II-VI Foundation Block Gift Program. Any opinions, findings, conclusions, or recommendations expressed in this material are those of the authors and do not necessarily reflect the views of the funding provider.

AUTHOR DECLARATIONS Conflict of Interest

The authors have no conflicts to disclose.

Author Contributions

Hemant Ghadi: Conceptualization (lead); Data curation (lead); Formal analysis (lead); Investigation (lead); Methodology (lead); Validation (lead); Visualization (lead); Writing – original draft (lead); Writing – review & editing (lead). **Evan Cornuellue**: Conceptualization (equal); Data curation (equal); Formal analysis (equal); Investigation (equal); Writing – review & editing (equal). **Joe F. Mcglone**: Conceptualization (equal); Formal analysis (equal); Investigation (equal); Writing – review & editing (equal). **Alexander Senckowski**: Investigation (equal); Resources (equal); Writing – review & editing (equal). **Shivam Sharma**: Investigation (equal); Resources (equal); Writing – review & editing (equal). **Man Hoi Wong**: Conceptualization (equal); Formal analysis (equal); Investigation (equal); Resources (equal); Visualization (equal); Writing – review & editing (equal). **Uttam Singisetti**: Conceptualization (equal); Investigation (equal); Resources (equal); Writing – review & editing (equal). **StevenA.Ringel**: Conceptualization (equal); Formal analysis (equal); Funding acquisition (equal); Methodology (equal); Resources (equal); Supervision (equal); Validation (equal); Visualization (equal); Writing – original draft (equal); Writing – review & editing (equal).

DATA AVAILABILITY

The data that support the findings of this study are available from the corresponding author upon reasonable request.

REFERENCES

1 H. Peelaers, J. L. Lyons, J. B. Varley, and C. G. Van de Walle, "Deep acceptors and their diffusion in Ga_2O_3," APL Mater. **7**(2), 022519 (2019).

2 A. T. Neal, S. Mou, S. Rafique, H. Zhao, E. Ahmadi, J. S. Speck, K. T. Stevens, J. D. Blevins, D. B. Thomson, N. Moser, K. D. Chabak, and G. H. Jessen, "Donors and deep acceptors in β-Ga_2O_3," Appl. Phys. Lett. **113**(6), 062101 (2018).

3 J. B. Varley, J. R. Weber, A. Janotti, and C. G. Van de Walle, "Oxygen vacancies and donor impurities in β-Ga_2O_3," Appl. Phys. Lett. **97**(14), 142106 (2010).

4 K. Iwaya, R. Shimizu, H. Aida, T. Hashizume, and T. Hitosugi, "Atomically resolved silicon donor states of β-Ga_2O_3," Appl. Phys. Lett. **98**(14), 142116 (2011).

5 H. Ghadi, J. F. McGlone, E. Cornuelle, A. Senckowski, S. Sharma, M. H. Wong, U. Singisetti, Y. K. Frodason, H. Peelaers, J. L. Lyons, J. B. Varley, C. G. Van de Walle, A. Arehart, and S. A. Ringel, "Identification and characterization of deep nitrogen acceptors in β-Ga_2O_3 using defect spectroscopies," APL Mater. **11**(11), 111110 (2023). 6 M. E. Ingebrigtsen, J. B. Varley, A. Yu. Kuznetsov, B. G. Svensson, G. Alfieri, A. Mihaila, U. Badstübner, and L. Vines, "Iron and intrinsic deep level states in Ga_2O_3," Appl. Phys. Lett. **112**(4), 042104 (2018).

7 P. Seyidov, J. B. Varley, Z. Galazka, T.-S. Chou, A. Popp, A. Fiedler, and K. Irmscher, "Cobalt as a promising dopant for producing semi-insulating β-Ga_2O_3 crystals: Charge state transition levels from experiment and theory," APL Mater. **10**(11), 111109 (2022).

8 P. Seyidov, J. B. Varley, J.-X. Shen, Z. Galazka, T.-S. Chou, A. Popp, M. Albrecht, K. Irmscher, and A. Fiedler, "Charge state transition levels of Ni in β-Ga_2O_3 crystals from experiment and theory: An attractive candidate for compensation doping," J. Appl. Phys. **134**(20), 205701 (2023).

9 M. H. Wong, C.-H. Lin, A. Kuramata, S. Yamakoshi, H. Murakami, Y. Kumagai, and M. Higashiwaki, "Acceptor doping of β-Ga_2O_3 by Mg and N ion implantations," Appl. Phys. Lett. **113**(10), 102103 (2018).

10 A. Armstrong, J. Caudill, A. Corrion, C. Poblenz, U. K. Mishra, J. S. Speck, and S. A. Ringel, "Characterization of majority and minority carrier deep levels in *p*-type GaN:Mg grown by molecular beam epitaxy using deep level optical spectroscopy," J. Appl. Phys. **103**(6), 063722 (2008).

11 A. Armstrong, A. R. Arehart, and S. A. Ringel, "A method to determine deep level profiles in highly compensated, wide band gap semiconductors," J. Appl. Phys. **97**(8), 083529 (2005).

12 B. E. Kananen, N. C. Giles, L. E. Halliburton, G. K. Foundos, K. B. Chang, and K. T. Stevens, "Self-trapped holes in β-Ga_2O_3 crystals," J. Appl. Phys. **122**(21), 215703 (2017). 13 Y. K. Frodason, K. M. Johansen, L. Vines, and J. B. Varley, "Self-trapped hole and impurity-related broad luminescence in β-Ga_2O_3," J. Appl. Phys. **127**(7), 075701 (2020). 14 S. Marcinkevicius and J. S. Speck, "Ultrafast dynamics of hole self-localization˘ in β-Ga_2O_3," Appl. Phys. Lett. **116**(13), 132101 (2020).

15 A. Hierro, D. Kwon, S. A. Ringel, S. Rubini, E. Pelucchi, and A. Franciosi, "Photocapacitance study of bulk deep levels in ZnSe grown by molecular-beam epitaxy," J. Appl. Phys. **87**(2), 730–738 (2000).

16 A. Hierro, D. Kwon, S. H. Goss, L. J. Brillson, S. A. Ringel, S. Rubini, E. Pelucchi, and A. Franciosi, "Evidence for a dominant midgap trap in n-ZnSe grown by molecular beam epitaxy," Appl. Phys. Lett. **75**(6), 832–834 (1999).

17 Y. Yao, S. Okur, L. A. M. Lyle, G. S. Tompa, T. Salagaj, N. Sbrockey, R. F. Davis, and L. M. Porter, "Growth and characterization of α-, β-, and ϵ-phases of Ga_2O_3 using MOCVD and HVPE techniques," Mater. Res. Lett. **6**(5), 268–275 (2018).

18 H. Ghadi, J. F. McGlone, E. Cornuelle, Z. Feng, Y. Zhang, L. Meng, H. Zhao, A. R. Arehart, and S. A. Ringel, "Deep level defects in low-pressure chemical vapor deposition grown (010) β-Ga_2O_3," APL Mater. **10**(10), 101110 (2022).

19 J. F. McGlone, H. Ghadi, E. Cornuelle, A. Armstrong, G. Burns, Z. Feng, A. F. M. A. Uddin Bhuiyan, H. Zhao, A. R. Arehart, and S. A. Ringel, "Proton radiation effects on electronic defect states in MOCVD-grown (010) β-Ga_2O_3," J. Appl. Phys. **133**(4), 045702 (2023).

20 H. Ghadi, J. F. McGlone, C. M. Jackson, E. Farzana, Z. Feng, A. F. M. A. Uddin Bhuiyan, H. Zhao, A. R. Arehart, and S. A. Ringel, "Full bandgap defect state characterization of β-Ga_2O_3 grown by metal organic chemical vapor deposition," APL Mater. **8**(2), 021111 (2020).

21 H. Ghadi, J. F. McGlone, Z. Feng, A. F. M. A. Uddin Bhuiyan, H. Zhao, A. R. Arehart, and S. A. Ringel, "Influence of growth temperature on defect states throughout the bandgap of MOCVD-grown β-Ga_2O_3," Appl. Phys. Lett. **117**(17), 172106 (2020). 22 R. Pässler, "Photoionization cross-section analysis for a deep trap contributing to current collapse in GaN field-effect transistors," J. Appl. Phys. **96**(1), 715–722 (2004). 23 A. Chantre, G. Vincent, and D. Bois, "Deep-level optical spectroscopy in GaAs," Phys. Rev. B **23**(10), 5335–5359 (1981).

24 J. M. Johnson, Z. Chen, J. B. Varley, C. M. Jackson, E. Farzana, Z. Zhang, A. R. Arehart, H.-L. Huang, A. Genc, S. A. Ringel, C. G. Van de Walle, D. A. Muller, and J. Hwang, "Unusual Formation of point-defect complexes in the ultrawide-bandgap semiconductor β-Ga_2O_3," Phys. Rev. X **9**(4), 041027 (2019).

25 E. Farzana, E. Ahmadi, J. S. Speck, A. R. Arehart, and S. A. Ringel, "Deep level defects in Ge-doped (010) β-Ga_2O_3 layers grown by plasma-assisted molecular beam epitaxy," J. Appl. Phys. **123**(16), 161410 (2018).

26 Z. Zhang, E. Farzana, A. R. Arehart, and S. A. Ringel, "Deep level defects throughout the bandgap of (010) β-Ga_2O_3 detected by optically and thermally stimulated defect spectroscopy," Appl. Phys. Lett. **108**(5), 052105 (2016). 27 B. R. Tak, M. Garg, S. Dewan, C. G. Torres-Castanedo, K.-H. Li, V. Gupta, X. Li, and R. Singh, "High-temperature photocurrent mechanism of β-Ga_2O_3 based metal–semiconductor–metal solar-blind photodetectors," J. Appl. Phys. **125**(14), 144501 (2019). 28 A. Singh Pratiyush, S. Krishnamoorthy, S. Vishnu Solanke, Z. Xia, R. Muralidharan, S. Rajan, and D. N. Nath, "High responsivity in molecular beam epitaxy grown β-Ga_2O_3 metal semiconductor metal solar blind deep-UV photodetector," Appl. Phys. Lett. **110**(22), 221107 (2017).

29 J. B. Varley, A. Janotti, C. Franchini, and C. G. Van de Walle, "Role of selftrapping in luminescence and p-type conductivity of wide-band-gap oxides," Phys. Rev. B **85**(8), 081109 (2012).

30 A. Alkauskas, M. D. McCluskey, and C. G. Van de Walle, "Tutorial: Defects in semiconductors—Combining experiment and theory," J. Appl. Phys. **119**(18), 181101 (2016). 31

H. J. Ghadi, J. F. McGlone, E. Farzana, A. R. Arehart, and S. A. Ringel, "Radiation effects on β-Ga_2O_3 materials and devices," in *Ultrawide Bandgap β-Ga_2O_3 Semiconductor: Theory and Applications*, edited by J. S. Speck and E. Farzana (AIP Publishing LLC), ISBN electronic: 978-0-7354-2503-3, ISBN print: 978-0-7354-2500-2, (2023).

32 V. I. Turchanikov, V. S. Lysenko, and V. A. Gusev, "Isothermal DLTS method using sampling time scanning," Phys. Status Solidi A **95**(1), 283–289 (1986).

33 P. Blood and J. W. Orton, *The Electrical Characterization of Semiconductors: Majority Carriers and Electron States* (Academic Press Limited, San Diego, CA, 1992). 34 C. Freysoldt, B. Grabowski, T. Hickel, J. Neugebauer, G. Kresse, A. Janotti, and C. G. Van de Walle, "First-principles calculations for point defects in solids," Rev. Mod. Phys. **86**(1), 253–305 (2014).

35 S. Poncé and F. Giustino, "Structural, electronic, elastic, power, and transport properties of β-Ga_2O_3 from first principles," Phys. Rev. Res. **2**(3), 033102 (2020). 36 C. Ma, Z. Wu, Z. Jiang, Y. Chen, W. Ruan, H. Zhang, H. Zhu, G. Zhang, J. Kang, T.-Y. Zhang, J. Chu, and Z. Fang, "Exploring the feasibility and conduction mechanisms of P-type nitrogen-doped β-Ga_2O_3 with high hole mobility," J. Mater. Chem. C **10**(17), 6673–6681 (2022).

37 E. Chikoidze, C. Sartel, H. Mohamed, I. Madaci, T. Tchelidze, M. Modreanu, P. Vales-Castro, C. Rubio, C. Arnold, V. Sallet, Y. Dumont, and A. Perez-Tomas, "Enhancing the intrinsic p-type conductivity of the ultra-wide bandgap Ga_2O_3 semiconductor," J. Mater. Chem. C **7**(33), 10231–10239 (2019).

38 E. Chikoidze, A. Fellous, A. Perez-Tomas, G. Sauthier, T. Tchelidze, C. TonThat, T. T. Huynh, M. Phillips, S. Russell, M. Jennings, B. Berini, F. Jomard, and Y. Dumont, "P-type β-gallium oxide: A new perspective for power and optoelectronic devices," Mater. Today Phys. **3**, 118–126 (2017).